

MIT Open Access Articles

Electron tunneling characteristics on La_{0.7}Sr_{0.3}MnO₃ thin-film surfaces at high temperature

The MIT Faculty has made this article openly available. **Please share** how this access benefits you. Your story matters.

Citation: Katsiev, Khabiboulakh et al. "Electron tunneling characteristics on La_{0.7}Sr_{0.3}MnO₃ thin-film surfaces at high temperature." Applied Physics Letters 95 (2009): 092106. © 2009 American Institute of Physics.

As Published: <http://dx.doi.org/10.1063/1.3204022>

Publisher: American Institute of Physics

Persistent URL: <http://hdl.handle.net/1721.1/67334>

Version: Final published version: final published article, as it appeared in a journal, conference proceedings, or other formally published context

Terms of Use: Article is made available in accordance with the publisher's policy and may be subject to US copyright law. Please refer to the publisher's site for terms of use.



Electron tunneling characteristics on $\text{La}_{0.7}\text{Sr}_{0.3}\text{MnO}_3$ thin-film surfaces at high temperature

Khajiboulakh Katsiev,¹ Bilge Yildiz,^{1,a)} Kavaipatti Balasubramaniam,² and Paul A. Salvador²

¹Department of Nuclear Science and Engineering, Massachusetts Institute of Technology, 77 Massachusetts Avenue, Cambridge, Massachusetts 02139, USA

²Department of Materials Science and Engineering, Carnegie Mellon University, 149 Roberts Engineering Hall, Pittsburgh, Pennsylvania 15213, USA

(Received 3 June 2009; accepted 21 July 2009; published online 1 September 2009)

We report on the electron tunneling characteristics on $\text{La}_{0.7}\text{Sr}_{0.3}\text{MnO}_3$ (LSM) thin-film surfaces up to 580 °C in 10^{-3} mbar oxygen pressure, using scanning tunneling microscopy/spectroscopy (STM/STS). A thresholdlike drop in the tunneling current was observed at positive bias in STS, which is interpreted as a unique indicator for the activation polarization in cation-oxygen bonding on LSM cathodes. Sr-enrichment was found on the surface at high temperature using Auger electron spectroscopy, and was accompanied by a decrease in tunneling conductance in STS. This suggests that Sr-terminated surfaces are less active for electron transfer in oxygen reduction compared to Mn-terminated surfaces on LSM. © 2009 American Institute of Physics.

[DOI: 10.1063/1.3204022]

Perovskite-type mixed ionic-electronic conductor (MIEC) oxides are widely used as solid oxide fuel cell (SOFC) cathodes,¹ and their surface structure plays an important role in the electrocatalytic activity for oxygen reduction (OR).^{2,3} A particularly interesting material in this context is $\text{La}_{(1-x)}\text{Sr}_x\text{MnO}_{3+\delta}$ (LSM)^{4,5}—an MIEC with poor ionic conductivity. The underlying OR mechanisms involving electronic and ionic charge transport on SOFC cathodes are not fully understood,² and the impact of different metal cations on the catalytic properties of the surface remains unclear.⁶ An improved understanding of the surface electronic and chemical state and its relation to the OR at the atomistic level is essential to the design of cathodes with enhanced electrocatalytic activity. In doing so, probing the surface electronic properties in conditions representative of the reaction temperatures and pressures is needed.⁷

We investigated the correlations of the surface composition of $\text{La}_{0.7}\text{Sr}_{0.3}\text{MnO}_3$ (LSM) model dense thin-films to their surface electronic structure and electron transport characteristics. We deployed an *in situ* approach combining surface sensitive probes of electronic structure and chemical state on the thin films—scanning tunneling microscopy and spectroscopy (STM/STS) and Auger electron spectroscopy (AES). Utilizing these surface sensitive probes, particularly the STM/STS, at as high temperatures and non-ultrahigh-vacuum (non-UHV) conditions is thus far unique, and facilitates to relate the chemical and electronic state of the model cathode surfaces closely to the reaction environment of operational SOFC cathodes.

$\text{La}_{0.7}\text{Sr}_{0.3}\text{MnO}_3$ polycrystalline dense thin films of 10–100 nm thickness were grown on single crystal (111) yttria-stabilized zirconia by pulsed laser deposition at 800 °C in 50 mTorr of O_2 , and subsequently cooled to room temperature in 300 Torr O_2 .⁸

The structural, electronic, and compositional characterizations were performed in a UHV surface science system

(by Omicron GmbH). The analysis chamber is equipped with a variable-temperature AFM/STM (Omicron VT25), retractable low-energy electron diffraction (LEED) optics, electron gun, and a cylindrical mirror energy analyzer for AES. Auger electron spectra were acquired using a normal incidence 4.8 keV electron beam. The samples were radiatively heated by a pyrolytic boron nitride heater during the annealing in oxygen for cleaning the surface and the high temperature STM/STS and AES experiments. A retractable oxygen doser equipped with a high precision leak valve was used for direct dosing the sample surface with oxygen during STM imaging and STS measurements. This setup allowed to create a 10^{-3} mbar oxygen pressure, P_{O_2} , localized in the vicinity of the sample's surface while the chamber base was at $P_{\text{O}_2} = 10^{-6}$ mbar. AES to probe the sample cleanliness were performed at $\sim 2 \times 10^{-10}$ mbar at ambient temperature. AES to identify the relative changes in the La, Sr, and Mn content on the surface were performed at $P_{\text{O}_2} = 10^{-6}$ mbar in the chamber at sample temperatures from 20 to 700 °C.

The *in situ* cleaning of the as-grown films was performed by heating the samples to 500 °C in oxygen at $P_{\text{O}_2} = 5 \times 10^{-7}$ mbar for 30 min, which resulted in a significant reduction of the carbon adsorbates below the detection limit of the AES energy analyzer. STM at room temperature and high temperatures was performed in the constant-current mode using 80%Pt-20%Ir tips, with the tunneling current, I , in the 0.1 to 1 nA range and the sample at a bias voltage, V , in the -1 to 3 V range. During the STS measurements, the bias voltage was varied from -3 to 3 V in 20 mV steps, with an acquisition time of 0.6 or 20 ms per voltage step for the I - V and dI/dV data, respectively. All the I - V curves discussed here represent an average behavior over the 15–20 subsequent spectra.

The STM performed on the 50-nm-thick LSM film at room temperature [Fig. 1(a)] showed a textured surface structure. Two types of grains coexisted, without an apparent crystallographic orientation in the topographic images. First is the large island-type flat grains, with a size distribution from 70 to 140 nm, and clearly distinguishable step edges.

^{a)}Author to whom correspondence should be addressed. Electronic mail: byildiz@mit.edu.

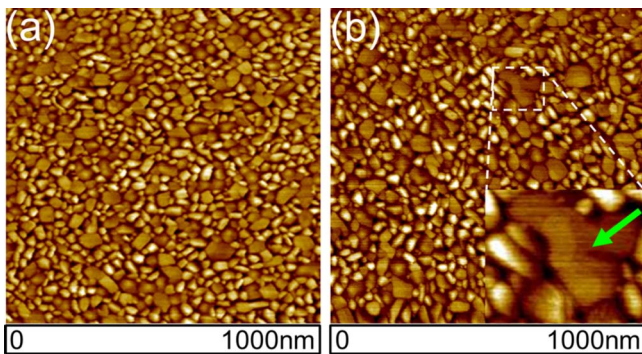


FIG. 1. (Color online) Topography ($1 \times 1 \mu\text{m}^2$) of the 50-nm-thick dense thin-film LSM surface imaged with tunneling conditions of 2 V and 1 nA at (a) room temperature in UHV and (b) 580 °C, $P_{\text{O}_2} = 10^{-3}$ mbar. The inset, $150 \times 137 \text{ nm}^2$, in (b) shows the step-edge resolution on the island-type flat grains (the location of the inset is shown by dashed lines).

The second type consists of smaller grains, with a size distribution from 30 to 50 nm. The overall peak-to-valley height difference is 6 nm. The LSM film structure did not evidently change via grain coarsening or surface roughening during the STM/STS experiments at 580 °C in $P_{\text{O}_2} = 10^{-3}$ mbar [Fig. 1(b)] lasting up to 24 h. The optimized conditions allowing for high resolution imaging, down to step edges [inset Fig. 1(b)] at high temperature in non-UHV conditions were obtained. This was necessary for the STS measurements to stably probe the electronic properties of the LSM surface. All results presented in this paper belong to this specific sample.

Temperature-dependent *in situ* AES measurement in $P_{\text{O}_2} = 10^{-6}$ mbar revealed enrichment of Sr and decrease of La on the surface [Fig. 2(a)], resulting in an overall 15%–27% increase in the (La+Sr)/Mn ratio at 600–700 °C [Fig. 2(b)]. Particularly due to the significant increase in the (La+Sr)/Mn ratio above 1.0 accompanied with the Sr-enrichment, we attribute this evolution to a thermodynamically favored Sr-rich phase on the LSM surface during the AES experiment conditions. This observation is consistent with prior experimental results which report Sr segregation on the LSM surface^{9,10} measured at room temperature in UHV conditions upon high temperature annealing in air, and often accompanied by changes in the Mn valence state,¹¹ although a Mn valence state change was not resolved in our AES data. Furthermore, these results are supported by recent *ab initio* hybrid density-functional calculations,¹² which predict the coexistence of (Sr,La)O and MnO_2 phases on the

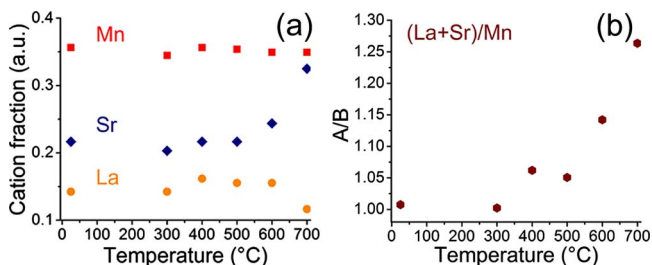


FIG. 2. (Color online) Temperature dependent AES in 10^{-6} mbar oxygen pressure revealed (a) Sr enrichment, accompanied by a decrease in La at the surface above 500 °C, while Mn remained unchanged. (b) (La+Sr)/Mn ratio showed an overall relative increase in the A site cations. The quantification in the AES data was performed based on the La_{MNN} , Sr_{LMM} , Mn_{LMM} , and O_{KLL} transitions. The error bar range in the experimental data was estimated to be <2%.

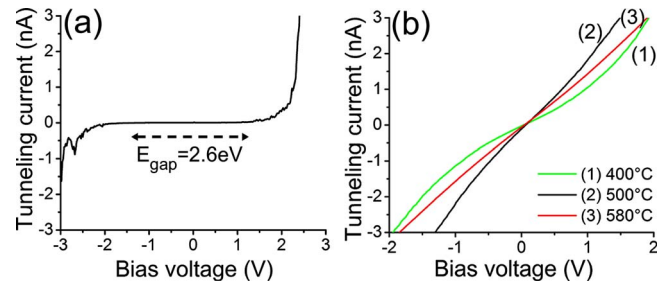


FIG. 3. (Color online) Tunneling current spectra acquired on the surface of the 50-nm-thick LSM at (a) room temperature and (b) 400, 500, and 580 °C with the acquisition time of 0.6 ms per voltage step.

surface at room temperature and the (Sr,La)O phase as energetically more favorable at 800 °C and $P_{\text{O}_2} = 0.2$ atm on LSM.

Electronic tunneling current on LSM surface exhibited a semiconductor-like band gap behavior at room temperature and a metallic nature at 400–580 °C [Figs. 3(a) and 3(b), acquisition time of 0.6 ms per voltage step]. An increase in the tunneling conductance was found as the temperature increased to 400 and 500 °C, followed by a decrease at 580 °C. The *I-V* data reverse to the band gap behavior upon cooling of the sample in oxygen to room temperature. The increase in the tunneling conductance reflected in the transition from a large band gap (2.6 eV) to metallic nature cannot be caused by the effect of the elevated temperature on a semiconductor.¹³ Thermal excitation at 400 °C is well below 2.6 eV energy and cannot enable the transition to a metallic conductance in this case. While yet uncertain, we hypothesize that this transition could be due to a structural transformation on the surface; for example, from an orthorhombic phase characterized by a strong Jahn–Teller distortion as an insulating paramagnetic state to a rhombohedral phase with a ferromagnetic metallic state.^{14,15} The subsequent decrease in conductance from 500 to 580 °C can result from the thermodynamically driven changes in the surface structure and composition of the LSM. While no diffraction pattern was observed by LEED in this work, we identified a chemical change associated with Sr-segregation and A-site/B-site ratio changes on LSM surface, as discussed above for the temperature-dependent AES results (Fig. 2).

Electronic conductance of the LSM is associated with the Mn cation and its oxidation state. A *p*-type conductivity in LSM arises as a result of hole-doping through the increase in $\text{Mn}^{4+}/\text{Mn}^{3+}$ ratio,¹⁶ which depends on the A-site cation substitution and oxygen nonstoichiometry. We attribute the decreasing tunneling conductance measured with STS at 580 °C (Fig. 3) to the evolution of a Sr-rich phase accompanied by the relative decrease of Mn on the surface as probed by AES at comparable conditions (Fig. 2). This result suggests that the A-site rich and Mn-poor surfaces are less active for electron exchange in OR on LSM.¹⁷

The STS measured within the range from -3 to $+3$ V with 20 ms acquisition time per voltage step at $P_{\text{O}_2} = 10^{-3}$ mbar and elevated temperatures revealed a sudden drop in the tunneling current at a positive threshold bias [Fig. 4(a)]. This differs from the STS spectra acquired with 0.6 ms per voltage step [Fig. 3(b)]. The threshold bias, V_{th} , decreased with increasing temperature, and was 2.6, 2.3, and 1.5 V at 400, 500, and 580 °C, respectively [Fig. 4(b)].

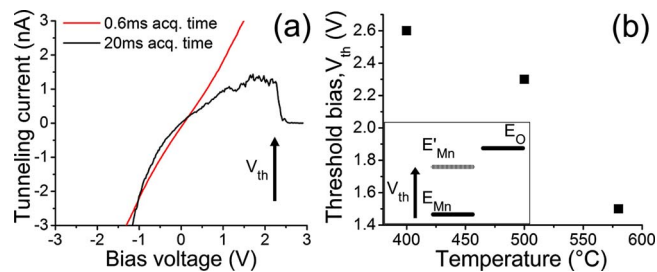


FIG. 4. (Color online) (a) Tunneling conductance spectra acquired on the surface of the 50-nm-thick LSM at 580 °C (acquisition time of 0.6 and 20 ms per voltage step) and (b) the threshold bias as a function of temperature. The inset in (b) schematically shows the cation energy levels (E_{Mn}) shifting upward (E'_{Mn}) at positive bias and approaching the oxygen electronic levels (E_O).

Similar threshold behavior was also observed on the 10- and 100-nm-thick LSM films (not reported here).

The acquisition-time-, temperature-, and bias-dependent character of the tunneling drop on LSM suggests that the underlying phenomenon is an activated chemical reaction; with the acquisition time-dependence related to the yield, and the temperature and bias dependence related to the activation of the reaction. Since the surface is expected to have oxygen vacancies at high temperature, but investigated in a P_{O_2} environment, we suggest that this chemical reaction might be a localized oxidation of the LSM surface induced by the tunneling bias. It is possible that the drop in the tunneling current can also be caused by the oxidation of Pt/Ir tip's apex. STM imaging and the STS I - V spectra with the 0.6 ms acquisition time was fully reproduced following the tunneling current drop in scans with a 20 ms acquisition time, thus suggesting that the tip was not altered.

While here we report this behavior originally for a perovskite surface at high temperature, a similar tip-induced nanometric oxidation accompanied by the drop in tunneling conductance was extensively studied for Si and GaAs surfaces at room temperature.^{18,19} The observation for the bias-induced oxidation was supported by an analytical model based on the Cabrera–Mott theory.²⁰ In the LSM surface region, positive bias leads to an upward bending of the electronic bands²¹ and shifts the cation electronic states to higher energy, as schematically shown in Fig. 4(b) inset. The bias-induced band bending can increase the catalytic activity, resulting in the oxygen chemisorption localized at the tip—LSM surface region at high temperature. The consequent formation of oxidized sites is a possible mechanism explaining the tunneling drop in STS shown in Fig. 4. Recent *ab initio* studies^{6,22} indicate that the favorable site for oxygen binding on LSM surface is atop Mn cation. The valence band maximum of LSM (from -3 to 0 eV) consists of Mn($3d$)-derived states that are split into t_{2g} and e_g bands.^{14,23} Due to the p -type conductivity of LSM, the electron transfer to oxygen should take place from the t_{2g} levels.²⁴ The upward shift in the relative energies [Fig. 4(b)] of these Mn($3d$)-derived states can increase the activity for the reaction with oxygen from the gas phase.^{25,26} Based on this mechanism, we suggest that the threshold bias, V_{th} , can serve as a unique probe of the activation polarization in cation-oxygen bonding on LSM cathode surface.

In summary, we investigated the electron tunneling characteristics on LSM thin-film surfaces using STM/STS up to 580 °C in oxygen gas environment. This is an original STM/

STS investigation of LSM at as high temperatures and non-UHV conditions close to the reaction environment of operational SOFC cathodes. A threshold-like drop in the tunneling current was observed at positive bias in STS at high temperature, and is interpreted as a unique indicator for the activation polarization in cation-oxygen bonding on the surface. AES revealed Sr-enrichment on the surfaces from 500 to 700 °C, and was accompanied by a decrease in tunneling conductance in STS. This suggests that the Mn-terminated surfaces are more active for electron transfer in OR compared to the Sr-rich surfaces on LSM. These findings can contribute to the atomic-scale understanding of the electrocatalytic properties on LSM cathodes, and serve as a key for the design of desirable cathodes for SOFCs.

We thank Department of Energy Office of Fossil Energy for financial support under Award No. DE-NT0004117, and Dr. Clemens Heske and Dr. Hoydoo You for constructive discussions. This work was performed in part at the Center for Nanoscale Systems, which is supported by the National Science Foundation under Award No. ECS-0335765.

- ¹S. C. Singhal, *Solid State Ionics* **135**, 305 (2000).
- ²S. B. Adler, *Chem. Rev. (Washington, D.C.)* **104**, 4972 (2004).
- ³F. S. Baumann, J. Fleig, M. Konuma, U. Starke, H.-U. Habermeier, and J. Maier, *J. Electrochem. Soc.* **152**, A2074 (2005).
- ⁴V. Brichzin, J. Fleig, H.-U. Habermeier, G. Cristiani, and J. Maier, *Solid State Ionics* **152–153**, 499 (2002).
- ⁵G. J. la O', B. Yildiz, S. McEuen, and Y. Shao-Horn, *J. Electrochem. Soc.* **154**, B427 (2007).
- ⁶Y.-L. Lee, D. Morgan, J. Kleis, and J. Rossmeisl, Proceedings of the 214th Meeting of the Electrochemical Society, Hawaii, USA, October 2008 (unpublished).
- ⁷A. Kolmakov and D. W. Goodman, *Catal. Lett.* **70**, 93 (2000).
- ⁸K. R. Balasubramaniam, S. Havlia, P. A. Salvador, H. Zheng, and J. Mitchell, *Appl. Phys. Lett.* **91**, 232901 (2007).
- ⁹H. H. Kumigashira, K. Horiba, H. Ohguchi, K. Ono, M. Oshima, N. Nakagawa, M. Lippmaa, M. Kawasaki, and H. Koinuma, *Appl. Phys. Lett.* **82**, 3430 (2003).
- ¹⁰R. Bertacco, J. P. Contour, A. Barthelemy, and J. Olivier, *Surf. Sci.* **511**, 366 (2002).
- ¹¹M. Backhaus-Ricoult, *Solid State Ionics* **177**, 2195 (2006).
- ¹²S. Piskunov, E. Heifets, T. Jacob, E. A. Kotomin, D. E. Ellis, and E. Spohr, *Phys. Rev. B* **78**, 121406(R) (2008).
- ¹³K. Seeger, *Semiconductor Physics: An Introduction*, 9th ed. (Springer, New York, 2004).
- ¹⁴A. Urushibara, Y. Moritomo, T. Arima, A. Asamitsu, G. Kido, and Y. Tokura, *Phys. Rev. B* **51**, 14103 (1995).
- ¹⁵M. P. de Jong, V. A. Dediu, C. Taliani, and W. R. Salaneck, *J. Appl. Phys.* **94**, 7292 (2003).
- ¹⁶C. Zener, *Phys. Rev.* **82**, 403 (1951).
- ¹⁷See EPAPS supplementary material at <http://dx.doi.org/10.1063/1.3204022> for the validation of the comparison of the STS and AES results.
- ¹⁸Y. Okada, Y. Iuchi, M. Kawabe, and J. S. Harris, Jr., *J. Appl. Phys.* **88**, 1136 (2000).
- ¹⁹D. Stievenard and B. Legrand, *Prog. Surf. Sci.* **81**, 112 (2006).
- ²⁰J. A. Dagata, F. Perez-Murano, G. Abadal, K. Morimoto, T. Inoue, J. Itoh, and H. Yokoyama, *Appl. Phys. Lett.* **76**, 2710 (2000).
- ²¹R. M. Feenstra, Y. Dong, M. P. Semtsiv, and W. T. Masselink, *Nanotechnology* **18**, 0444015 (2007).
- ²²Y. Choi, M. C. Lin, and M. Liu, *Angew. Chem., Int. Ed.* **46**, 7214 (2007).
- ²³A. Chikamatsu, H. Wadati, H. Kumigashira, M. Oshima, A. Fujimori, N. Hamada, T. Ohnishi, M. Lippmaa, K. Ono, M. Kawasaki, and H. Koinuma, *Phys. Rev. B* **73**, 195105 (2006).
- ²⁴H. Kamata, Y. Yonemura, J. Mizusaki, H. Tagawa, K. Narayato, and T. Sasamoto, *J. Phys. Chem. Solids* **56**, 943 (1995).
- ²⁵Ph. Avouris, R. E. Walkup, A. R. Rossi, H. C. Akpati, P. Nordlander, T.-C. Shen, G. C. Abeln, and J. W. Lyding, *Surf. Sci.* **363**, 368 (1996).
- ²⁶O. Bikondoa, C. L. Pang, R. Ithnin, C. A. Muryn, H. Onishi, and G. Thornton, *Nature Mater.* **5**, 189 (2006).